fMRI time series analysis based on stationary wavelet and spectrum analysis*

ZHI Lianhe[1,2,3], ZHAO Xia[4], SHAN Baoci[1**], PENG Silong[5], YAN Qiang[1], YUAN Xiuli[1] and TANG Xiaowei[1,6]

(1. Key Laboratory of Nuclear Analysis Techniques, Institute of High Energy Physics, Chinese Academy of Sciences, Beijing 100049, China; 2. Graduate School of Chinese Academy of Sciences, Beijing 100049, China; 3. Department of Physics, Zhoukou Normal University, Zhoukou 466100, China; 4. Research Imaging Center, University of Texas Health Science Center, San Antonio, Texas 78229, USA; 5. National ASIC Design and Engineering Center, Institute of Automation, Chinese Academy of Sciences, Beijing 100049, China; 6. Department of Physics, Zhejiang University, Hangzhou 310027, China)

Received February 16, 2006; revised March 30, 2006

Abstract The low signal to noise ratio (SNR) of functional MRI (fMRI) prefers more sensitive data analysis methods. Based on stationary wavelet transform and spectrum analysis, a new method with high detective sensitivity was developed for analyzing fMRI time series, which does not require any prior assumption of the characteristics of noises. In the proposed method, every component of fMRI time series in the different time-frequency scales of stationary wavelet transform was discerned by the spectrum analysis, then the components from noises were removed using the stationary wavelet transform, finally the components of real brain activation were detected by cross-correlation analysis. The results obtained from both simulated and *in vivo* visual experiments illustrated that the proposed method has much higher sensitivity than the traditional cross-correlation method.

Keywords: fMRI, stationary wavelet transform, spectrum analysis, data analysis.

Functional magnetic resonance imaging (fMRI) based on the blood-oxygenation-level -dependente (BOLD) contrast has rapidly become a powerful tool for exploring the human brain functions by virtue of its noninvasiveness, repeatability and excellent temporal-spatial resolution[1]. Unfortunately, the amplitude change of paradigm responsive signal (PRS) in fMRI due to the paradigm stimulation is only 1%—5% at 1.5 T[2,3], in addition to noises such as random noise and baseline drift[3—6], which makes the analysis procedure more complicated. So removing noises and enhancing sensitivity are one of the important goals of fMRI analysis.

A variety of methods have been developed for analyzing fMRI data sets, which are classified by many researchers[3,7—9] into two categories: model-driven method and data-driven method. The typical model-driven method is general linear model (GLM)[10]. The advantage of GLM is its ability of modeling the effects of many noises, for example, low frequency drift, and eliminating them. However, GLM needs to make prior assumption on the components of the fMRI BOLD signals. For example, the low frequency drift is simulated by the discrete cosine function and random noise is considered as Gaussian distribution in GLM. Thus the validity of the GLM depends on the extent to which the data satisfies the underlying assumptions. In contrast with the model-driven method, the data-driven method, such as fuzzy clustering analysis[11], principal component analysis[12], independent component analysis[13], does not need any prior hypothesis of paradigm or noises. The data-driven method will be more and more prevailing in the future due to its higher efficiency on the event-related fMRI experiments that will be increasingly dominate the fMRI area. However, it is difficult to give a physiological interpretation and a statistical significance level to the activated results detected by the data-driven methods.

As an analysis tool, wavelet transform has been widely used in fMRI analysis[14]. Using the traditional denoising method of wavelet transform to remove noises of fMRI series in stationary wavelet domain has been reported[14,15]. However, this method only involvs random noise, not including the baseline drift. There were reports[6,16,17] on removing the

* Supported by National Natural Science Foundation of China (Grant No. 30570508) and National Basic Research Program of China (2006CB705700)

** To whom correspondence should be addressed. E-mail: shanbc@ihep.ac.cn

baseline drift from fMRI series based on the discrete wavelet transform. However, because the frequency attribute of the baseline drift is poorly understood[6], and the time-frequency scales of the baseline drift cannot be exactly predicted, the way to remove the baseline drift in these literatures was tentative. Instead of using the existing wavelet, Von Tscharner et al.[18] designed a set of new wavelets whose frequency bands were equal to that of the paradigm to optimize analysis of fMRI. It is well known that selecting the suitable wavelet base is a critical and complex issue in wavelet analysis, as is limited by many other factors besides the frequency. For the fMRI analysis, the suitable wavelet base should be selected from the analysis results of the simulated data by different wavelets, but their study just lacked this.

In this article, we present a novel method for fMRI time series analysis based on the wavelet transform and spectrum analysis. Owing to the property of multiresolution analysis[19], wavelet transform can partition the components with the different frequency bands of a signal into the different time-frequency scales. So via wavelet transform the different components in fMRI time series of each pixel, e.g. the high frequency random noise, the low frequency baseline drift and the paradigm responsive signal (PRS) with the frequency in between those of noise and drift, can be partitioned into the different scales. Thus, after the time-frequency scales in which the simulated PRS exists are discerned by the spectrum analysis, random noise and baseline drift can be removed from the fMRI time series by way of eliminating the scales in which the noises exist when wavelet is reconstructed, finally the activated pixel can be detected by the cross-correlation analysis. As long as the frequencies of PRS and noises are not overlapped, both random noise and baseline drift can be removed altogether. Because the stationary wavelet transform has the property of time shift invariance that is important to the spectrum analysis and time series analysis[20], this transform was utilized to analyze fMRI time series in this study.

1 Materials

1.1 *in vivo* visual fMRI experiment

Three young right-handed subjects participated in a visual fMRI experiment with a block-design paradigm. There were two kinds of stimulating blocks, one was the task-related block which was a checkerboard pattern flashing with frequency of 8 Hz, the other was the rest-related block which was the white board. The paradigm design or stimulus input function was as follows: first was a rest block lasting for 80 s, then four task blocks for 10 s each and four rest blocks for 30 s each alternated, last was the rest block for 16 s. The experiments were carried out with a 1.5 T whole body scanner (Sonata, Siemens, Germany). Functional images were obtained using a BOLD T_2^*-weighted gradient-echo EPI sequence. The technical parameters were as follows: TR = 2000 ms, TE = 50 ms, flip angle 90°, field of view 22×22 cm^2, matrix size 64×64, in-plane resolution 3.44 mm, 20 slices covering the whole brain and paralleling to the AC-PC line, slice thickness 6 mm, slice gap 1.2 mm. A total of 128 volumes of whole brain functional images were acquired from each subject.

1.2 computer simulated fMRI dataset

In our experiment, the way to simulate dataset was similar to the previously reported[3,5,7,9]. A base image (displayed in Fig. 1) was replicated 128 times representing 128 timepoints of the baseline series, to which the Gaussian noise, low frequency drift, and PRS time series were added. The base image was obtained by averaging first 35 images of the first subject in the visual experiment, before averaging these images were all spatially realigned and normalized using SPM99 software[21]. Mean of the simulated Gaussian noise series was zero and standard deviation was 1. Low frequency drifts were simulated using first-degree polynomial, which has different amplitudes for each pixel and a normal distribution with zero mean and standard deviation 1. The simulated PRS series was defined as a stimulus input function convolved with the hemodynamic response function based on a linear time-invariant system[3,22]. Here, stimulus input function is the same as that of the *in vivo* visual experiment, hemodynamic response function was the difference of two gamma functions[23]. The amplitudes of PRS, low frequency drift, and noise level were adjusted to generate the simulated datasets with the specific contrast to noise ratio (CNR) and the fixed drift to noise ratio (DNR) 0.85[5]. The CNR is the ratio of the amplitude of the paradigm responsive signal to the standard deviation of the Gaussian noise[5,7,9]. The DNR is the ratio of the amplitude of baseline drift to standard deviation of the Gaussian noise[5]. The four simulated activated areas contained

25, 36, 49, 64 pixels respectively, shown in Fig. 1.

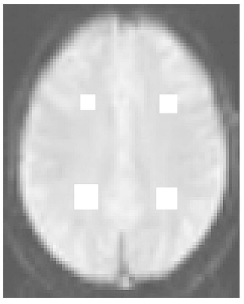

Fig. 1. The base image and the positions of four simulated activated areas (the white boxes).

2 Method

2.1 Stationary wavelet transform

Wavelet transform is to approach a signal in terms of a wavelet family, in such transform the wavelets act as sine and cosine functions in Fourier transform, and the wavelet family can be obtained by dilating and translating a mother wavelet and a scaling function. In the language of signal processing, the wavelet and the scaling function are equivalent to a high-pass and a low-pass filter respectively, the first level wavelet decomposition is to extract the high frequency component d_1 and low frequency component a_1 from the original signal a_0 through filtering and binary decimation. Similarly, the second level decomposition is to extract d_2 and a_2 from low frequency component a_1. If decomposing j times, the $j+1$ time-frequency-scale components $d_1 \cdots d_j$, a_j of a_0 in turn can be extracted, as is called the multiresolution analysis of wavelet transform[19]. Binary decimation causes shift variance of transform, so the stationary wavelet transform modifies the filters instead of using decimation to keep the property of shift invariance. Therefore, we used the stationary wavelet transform to analyze fMRI series and the programs we used are coded by the wavelet toolbox of Matlab6.5 software[24]. Based on the results obtained from simulated data below, sym4 is chosen as the wavelet base, which is approximately symmetry wavelet with compact support. In the practical application, the symmetry can keep phrase linear and the compact support can efficiently reduce the boundary effects of wavelet transform.

2.2 Detecting activated signals

The first and foremost step of our method is to discern how the components with the different frequency bands in fMRI series distribute in the different time-frequency scales of the stationary wavelet transform, which was fulfilled by using spectrum analysis and the simulated PRS. Spectrum of PRS (displayed in Fig. 2(a)) indicates that main frequency components of PRS are 0.025 Hz and 0.05 Hz. By conducting the stationary wavelet decomposition of the PRS for 7 levels and single-level reconstruction of the decomposition coefficients in every scale, the signal of total 8 time-frequency scales was gained. The frequency spectra of signals d_3, d_4 and d_7 are displayed respectively in Fig. 2(b), (c) and (d), the rest are not displayed because of the low energy. It is easy to see from Fig. 2 that the energy of the PRS mainly distributes in d_3 and d_4 scales after wavelet transform.

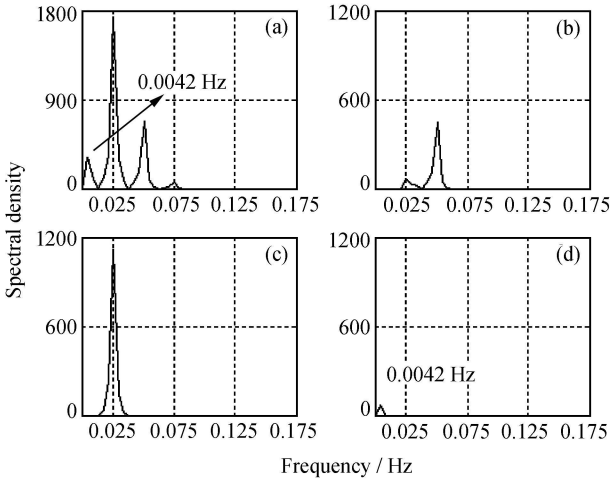

Fig. 2. Frequency spectrum of the simulated PRS and frequency spectra of the signals of d_3, d_4 and d_7 from PRS via stationary wavelet composition and single-level reconstruction.

The second step of our method is to remove the noises. Based on the analysis result in the first step, we decomposed the simulated and experimental data by stationary wavelet transform, and reconstructed the decomposition coefficients only in d_3 and d_4 scales because the components of the PRS exist in these scales. The coefficients in other scales that stand for the noises were discarded. The coefficient in d_7 scale was also discarded because the energy of the PRS component was low and especially, because of baseline drift overlapped in this scale[4]. The resultant reconstruction signal was the signal with less noise. So the way to remove the noises by our method is very simple.

The last step is to use the cross-correlation analy-

sis method to detect the activated pixels. We chose the reconstruction signal from d_3 and d_4 of PRS as the reference signal, and conducted the cross-correlation analysis of the reference signal with the reconstruction signal of simulated and experimental data respectively. In order to reduce the boundary effects of wavelet transform, we deleted the first 10 and the last 18 time-point data from reference signal and also from the reconstruction signal of simulated and experimental data, and used the remaining 100 time-point data for cross-correlation analysis. To test the significance level α of the correlation coefficient r, we performed Fisher's Z transformation[25] $z=\frac{\sqrt{N-3}}{2}\ln\frac{1+r}{1-r}$ to convert the r to a z-value which follows a normal distribution, where N is the dimension of sequence. Finally, as a comparison, we also conducted the cross-correlation analysis of the PRS with both simulated and experimental data, the dimension of each time series was also chosen as 100. For a short description, this method was called M1 while the cross-correlation method under the framework of the stationary wavelet transform was called M2.

3 Analysis results

3.1 Simulated data

To make the simulated data closely approach the real fMRI data, the parameters of the simulated datasets were as follows[7,9]: the noise level of each pixel was 2% of its own baseline value, the amplitude of activated pixel was 1.5%, 2.0%, 3.0%, and 4% of its own baseline value, the corresponding CNR was 0.75, 1.0, 1.5 and 2.0 respectively. In order to effectively remove the pixels outside the brain region, the pixels whose values smaller than one-fifth of the maximum pixel value in the image were filtered out for both simulated and experimental data before processing[9]. Spatial pixel-cluster of 5 was chosen for the spatial activated region[7]. Table 1 summarizes results obtained with two methods at the different CNR levels when significance level $\alpha=0.0001$. Fig. 3 gives the activated maps of M1 (the first row) and M2 (the second row) at the CNR levels of 1.0 (the first column), 1.5 (the second column) and 2.0 (the third column) when significance level $\alpha=0.0001$ while Table 2 gives the numbers of correctly detected activated pixels of two methods at the different significance level α when CNR=1.0. From Table 1, Fig. 1 and Table 2 can be seen that as the CNR increases, the number of correctly detected pixels by two methods increases, but under the condition of the same CNR, the number of correctly detected pixels by M2 is always bigger than that by M1, which is even obvious from the result at CNR=0.75 in Table 1 and in Fig3. (a) and (d). And more important is, the maximum z-value and mean of z-value of correctly detected pixels by M2 is always much bigger than those obtained by M1. On the other hand, as the Table 2 indicates, as the significance level α increases, the number of correctly detected pixels by two methods increases, but under the condition of the same significance level α, the number of correctly detected pixels by M2 is always bigger than that by M1, particularly when α is small. Furthermore, when significance level α is very small, M2 can detect almost the whole preset activated pixels. From mentioned above we can say that M2 has a much stronger detection ability, and is much more sensitive than M1.

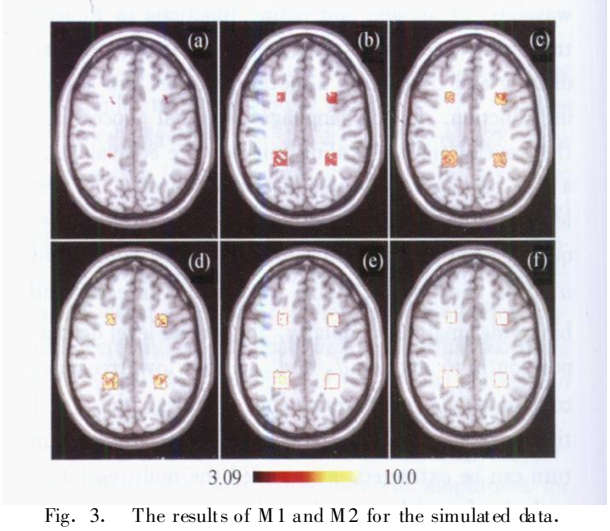

Fig. 3. The results of M1 and M2 for the simulated data.

Table 1. Comparison of two methods at different CNR

CNR		Total detected numbers	Correctly detected activated numbers (z max z mean)
0.75	M1	0	0(0 0)
	M2	145	137(11.27 6.41)
1.0	M1	23	23(5.66 4.45)
	M2	172	163(12.81 7.38)
1.5	M1	158	158(7.37 5.26)
	M2	190	174(15.08 10.40)
2.0	M1	174	174(9.20 6.51)
	M2	177	174(18.11 12.71)

($\alpha=0.0001$, the preset total activated pixels number is 174)

Table 2. Comparison of two methods at different significance level α

Significance level α	0.00001	0.0001	0.001	0.01
Correctly detected activated pixels (M1)	0	23	83	143
Correctly detected activated pixels (M2)	153	163	169	173

(CNR= 1.0, the preset total activated pixels number is 174)

3.2 Visual fMRI experiment

The imaging data of three subjects were first transformed into the analytic form by using SPM2[21], then spatially realigned and normalized into stereotaxic atlas space of Talairach[26], the pixels outside the brain region was removed using the same method as that for the simulated data, the sequence of each pixel was finally subject to processing by the methods of M1 and M2 respectively. The significance level of two method is $\alpha = 10^{-6}$ (approximately Bonferroni correction[6]). Limited by the length of paper, Fig. 4 only gives the activated maps at Talairach $z = 0$ mm. The first, second and third rows are corresponding to Subject 1, Subject 2 and Subject 3 respectively. The first column is the results of M1 with the spatial threshold 10, the second is the results of M2 with spatial threshold 10, and the third is results of M2 with spatial threshold 20. It can be seen from Fig. 4 that, although the activated area detected by M1 are all located in the areas of visual cortex, M2 can also detect these activated areas, and these activated areas detected are much larger than those by M1. So, as far as the number of detected activated pixels is concerned we can say that M2 is more sensitive than M1. On the other hand, as the colourbar indicated, in the activated areas commonly detected by M1 and M2, the z-value detected by M2 is always bigger than that by M1, this contrast can be even seen from the activated maps of Subject 1 and Subject 3. Therefore, M2 is more sensitive than M1 from the viewpoint of z-value in activated areas. However, it can also be seen from Fig. 4(b) and Fig. 4(e) that due to the high sensitivity of M2 a few activated pixels detected by M2 are not in the area of visual cortex. But the z-values of these pixels are very small compared with those in visual activated areas, and when spatial threshold is 20 most of these pixels are deleted (Fig. 4(c), (f)). In a word, the results of the visual experimental data again justified that M2 is a more sensitive method.

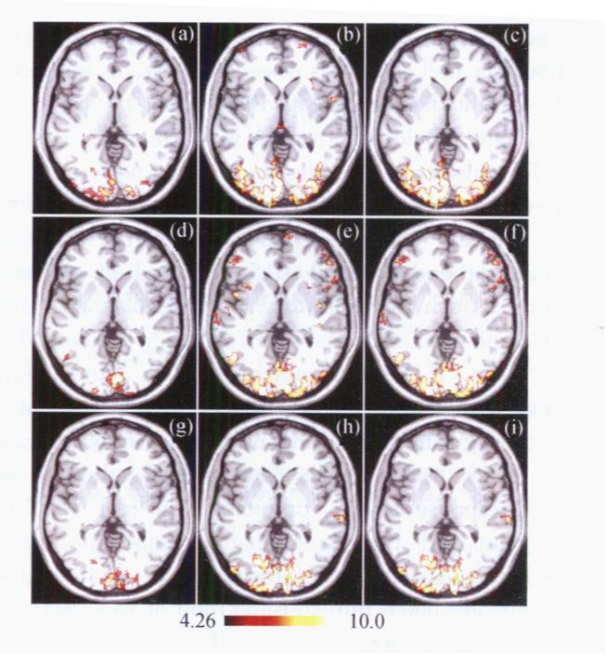

Fig. 4. The results of M1 and M2 for the visual experimental data.

4 Discussion and conclusions

A simple and novel method-fMRI time series analysis based on stationary wavelet and spectrum analysis—for analyzing fMRI time series is introduced. Compared with the traditional cross-correlation, the proposed method significantly increases the detection sensitivity when analyzing the simulated and experimental data. The advantage of this method stems from its stronger capacity of removing both random noise and baseline drift.

Based on the stationary wavelet transform and spectrum analysis, if the frequencies of PRS and noises are not overlapped, the proposed method can remove noises efficiently and relatively thoroughly, regardless of what distribution the random noise follows and how much the frequency of baseline drift is. So, there is no need to make assumptions on the property of noises or tentatively searching for the time-frequency scale of baseline drift in the wavelet domain. In addition, it should be particularly noted that the proposed method is not confined to analyzing the fMRI data. The time series of other images, such as electroencephalograph (EEG), magnetoencephalograph (MEG), can also be processed by the proposed method after slightly adapting, so the proposed method is promising in many signal processing areas.

However, in order to use the proposed method

validly and efficiently, the following conditions should be met as best as possible. First, as mentioned above, the frequencies of PRS when designing the paradigm should not overlap with those of noises in fMRI time series. Besides the thermal noise, the other serious noise in fMRI time series arises from physical sources, namely scanner drift with frequency ranged around 0.0—0.015 Hz, and physiological sources, such as respiratory with frequency of about 1 Hz and cardiac cycles with frequency of about 0.25 Hz[3, 4, 27]. If the frequency of the PRS is in the same range with that of noise, the PRS is very difficult to be distinguished from the noise. Secondly, because the delay between the experimental stimulus and brain response is very common in the real fMRI experiment and the hemodynamic response function used to construct the reference signal in our method has already taken into consideration of this delay[23], it is not recommended to use other analyzing method without considering the time delay other than cross-correlation analysis when using the proposed method.

Acknowledgments The authors are grateful to the reviewers for their significant and constructive comments and suggestions, which greatly improved the article.

References

1 Ogawa S., Lee T. M., Kay A. R. et al. Brain magnetic resonance imaging with contrast dependent on blood oxygenation. Proc. Natl. Acad. Sci. USA, 1990, 87(24): 9868—9872.
2 Bandettini P.A., Jesmanowicz A., Wong E.C. et al. Processing strategies for time-course data sets in functional MRI of the human brain. Magn. Reson. Med., 1993, 30: 161—173.
3 Hossien-Zadeh G. A., Soltanian-Zadeh H., and Ardekani A. Multiresolution fMRI activation detection using translation invariant wavelet transform and statistical analysis based on resampling. IEEE. Trans. Med. Imaging, 2003, 22(3): 302—314.
4 Smith A. M., Lewis B. K., Ruttimann U. E. et al. Investigation of low frequency drift in fMRI signal. NeuroImage, 1999, 9(5): 526—533.
5 Lowe M. J. and Russell D. P. Treatment of baseline drifts in fMRI time series analysis. Journal of Compute Assisted Tomography, 1999, 23(3): 463—473.
6 Tanabe J., Miller D., Tregellas J. et al. Comparison of detrending method for optimal fMRI preprocessing. Neuroimage, 2002, 15(4): 902—907.
7 Yee S. H. and Gao J. H. Improved detection of time windows of brain responses in fMRI using modified temporal clustering analysis. Magn. Reson. Imaging, 2002, 20(1): 17—26.
8 Lu Y. L., Jiang T. Z. and Zang Y. F. Region growing method for the analysis of functional MRI data. NeuroImaging, 2003, 20(1): 455—465.
9 Zhao X., Glahn D., Tan L. H. et al. Comparison of TCA and ICA techniques in fMRI data processing. J. Magn. Reson. Imaging, 2004, 19(4): 397—402.
10 Friston K. J., Holmes A. P., Worsley K. J. et al. Statistical parametric maps in functional imaging: a general linear approach. Human Brain Mapping, 1995, 2(4): 189—210.
11 Baumgartner R., Windischberger C. and Moser E. Quantification in functional magnetic resonance imaging: fuzzy clustering vs. correlation analysis. Magn. Reson. Imaging, 1998, 16(6): 115—125.
12 Lai S. H. and Fang M. A novel local PCA-based method for detecting activation signals in fMRI. Magn. Reson. Imaging, 1999, 17(6): 827—836.
13 McKeown M. J., Makeig S., Brown G. G. et al. Analysis of fMRI data by blind separation into independent spatial components. Human Brain Mapping, 1998, 6(3): 160—188.
14 Bullmore E., Fadili J., Maxim V. et al. Wavelets and functional magnetic resonance imaging of the human brain. NeuroImage, 2004, 23(1): S234—S249.
15 Alexander M. E., Baumgartner R., Windischberger C. et al. Wavelet domain de-noising of time-courses in MR image sequences. Magn. Reson. Imaging, 2000, 18: 1129—1134.
16 Meyer F. G. and McCarthy G. Estimation of baseline drift in fMRI. http://ece-www.colorado.edu/~fmeyer/Pub/ipmi01.pdf [2005 12 12]
17 Meyer F. G. Wavelet-based estimation of a semiparametric generalized linear model of fMRI time-series. IEEE Trans. Med. Imaging, 2003, 22(3): 315—322.
18 Von Tscharner V. and Thulborn K. R. Specified-resolution wavelet analysis of activation patterns from BOLD contrast fMRI. IEEE Trans. Med. Imaging, 2001, 20(8): 704—714.
19 Mallat S. G. A theory of multiresolution signal decompositions: the wavelet transform. IEEE Trans. Pattern Anal. Machine Intell., 1989, 11(7): 674—693.
20 Nason G. P. and Silverman B. W. The stationary wavelet transform and some statistical applications. In: Wavelet and Statistics, Lecture Notes in Statistics. Berlin: Springer Verlag, 1995, 281—300.
21 http://www.fil.ion.ucl.uk/spm. [2005 12 12]
22 Friston K. J., Jezzard P. and Turner R. Analysis of functional MRI time-series. Human Brain Mapping, 1994, 1(2): 153—171.
23 Friston K. J., Fletcher P., Josephs O. et al. Event-related fMRI: characterizing differential response. Neuroimage, 1998, 7(1): 30—40.
24 Hu C. H., Li G. H., Liu T. et al. Based on Matlab 6.x the System Analysis and Design—Wavelet Analysis. 2nd ed. Xi'an: XiDian University Press, 2004, 50.
25 Ardekani B. A. and Kanno I. Statistical methods for detecting activated regions in functional MRI of the brain. Magn. Reson. Imag., 1998, 16(10): 1217—1225.
26 Talairach J. and Tournoux P. Co-planar Stereotaxic Atlas of the Human Brain. New York: Thieme Medical Publishers, 1988, 1—110.
27 Frackowiak R. S. J., Friston K. J. and Frith C. D. Human Brain Function. Amsterdam: Academic Press, 1997.